ADVANCED FUNCTIONAL MATERIALS

Optical Control and Patterning of Gold-Nanorod–Poly(vinyl alcohol) Nanocomposite Films**

By *Jorge Pérez-Juste*,* *Benito Rodríguez-González*, *Paul Mulvaney*, and *Luis M. Liz-Marzán**

Gold nanorods with well-defined aspect ratios are homogeneously incorporated within poly(vinyl alcohol) thin films and subsequently aligned by heating and stretching the nanocomposite films. The spatial alignment of the nanorods is directly proved using transmission electron microscopy. The polarization-dependent optical response of the rods is measured and compared with a dipole model. Excellent agreement is found. Additionally, irradiation of the film with nanosecond laser pulses (1064 nm) leads to selective reshaping of the nanorods into nanospheres, and we demonstrate that this effect can be used to micropattern optical structures into the films.

1. Introduction

The unusual optical properties of metal nanoparticles have long been studied and exploited for practical purposes, the most ancient cases being those related to decorative glasses,[1] such as mosaics in churches. However, these applications have expanded more recently to include completely new fields such as microelectronics and biotechnology. The interest in such optical properties arises not only from the bright, visible colors that can be obtained,[2] but also because these colors can be tuned by the fine control of several parameters, such as particle size and shape, aggregation state, or the nature of the surroundings.[3] Research has long been hampered by the fact that metal particles usually grow as well-defined, facetted, spheroidal particles. Earlier efforts at modifying the optical properties of gold nanocrystals examined the role of particle size[4,5] and surface damping, dielectric[6] and metal shells,[3] and even dielectric-core–gold-shell particles,[7] which can result in tunable IR plasmon modes. The recent development of matrix[8,9] and surfactant-templated[10,11] syntheses for non-spherical geometries and other more complex morphologies has opened up many new research possibilities. In particular, the emphasis has shifted to the controlled generation of spatially organized structures and coupled-plasmon modes for information transmission in sub-wavelength devices.

Polarization effects provide a useful method for modulating the optical response of light in materials. Metal nanorods provide an interesting alternative to conventional, organic polarizers because of their enormous absorption coefficints and hence absorption coefficients, tunable peak positions, and higher photostability. For example, to date, gold and silver rods show little or no reactivity towards molecular oxygen during irradiation; in contrast, many complex, organic optical materials are slowly degraded by such treatment.

A necessary intermediate step between the synthesis of metal nanoparticles and their use in practical devices is their organization within solid matrices, such as polymers, glasses, or ceramics. Such combinations of a solid matrix with nanometer-sized components of a different material are often termed nanocomposites. Two main approaches have been traditionally followed for the preparation of nanocomposites containing metal nanoparticles, involving either the direct, in-situ formation of the nanoparticles within the matrix, or the transfer of pre-synthesized particles into the matrix. As usual, each method has its own advantages and disadvantages. The in-situ formation of particles within the matrix of interest[12–14] is often simple and just requires the reduction of metal ions by thermal or photochemical methods, but rigorous control of particle size, composition, morphology, and, in particular, the shape of the resultant nanoparticles, is very difficult. On the other hand, pre-synthesized nanoparticles can be tailored by means of the various colloid-chemistry techniques currently available, so that many more types of doped structures can be envisaged. For example, rods, ellipsoids, cubes, and other non-spherical shapes can be employed, and more complex core–shell, surface-functionalized particles, chromophore-derivatized metal particles, and metal–semiconductor composite particles can be used to dope the matrix and modify the optical behavior of the host matrix. A disadvantage of this second approach is that surface modification of these ex-situ synthesized materials is usually required to allow dispersion of the particles in the chosen matrix material, to ensure that aggregation during the pro-

[*] Dr. J. Pérez-Juste, Prof. L. M. Liz-Marzán, B. Rodríguez-González
Departamento de Química Física, Universidade de Vigo
E-36310 Vigo (Spain)
E-mail: juste@uvigo.es; lmarzan@uvigo.es
Prof. P. Mulvaney
Chemistry School, University of Melbourne
Parkville, VIC 3010 (Australia)

[**] We thank A. Sánchez-Iglesias for assistance with chemical synthesis. We also thank Prof. H. Michinel and Prof. J. Domînguez for granting access to a nanosecond laser and a polarizing optical microscope, respectively. Financial support from the Spanish Xunta de Galicia (Project no. PGIDIT03TMT30101PR), the Ministerio de Educación y Ciencia/FEDER (Project MAT2004-02991), and the ARC (Grant DP0344356) are gratefully acknowledged. Supporting Information is available from WileyInterscience (www.wileyinterscience.com) or from the author.

 DOI: 10.1002/adfm.200400591

cessing stage (polymerization, sol–gel transition, etc.) is prevented.[15–17]

Polymers offer a suitable matrix for the fabrication of composites with polarization-dependent optical properties. Preliminary work related to such composite materials has been published by Dirix et al.[18] using polyethylene films containing *spherical* silver nanoparticles. The films were drawn in a hot shoe, leading to the alignment of nanoparticle aggregates into necklaces or chains, which exhibited polarization-dependent optical responses. A more refined procedure has been utilized by Van der Zande et al.,[19] who prepared thin films of gold nanorods dispersed in poly(vinyl alcohol) (PVA) by simply drying a colloid in the presence of dissolved PVA. A similar procedure was adopted by Mulvaney and co-workers[20] with silver nanorods, and they demonstrated the possibility of patterning by the selective melting of the rods into spheres by laser irradiation.

Herein, we present a study of the structure and optical properties of PVA–Au-nanorod composite films in which monodisperse nanorods with different aspect ratios were used, and compare the results to theoretical predictions using the Mie-Gans model for prolate ellipsoids. We also show that rod-to-sphere transformation is possible with very good spatial resolution, simply by irradiation with 1064 nm nanosecond laser pulses in the presence of a suitable template.

2. Results and Discussion

2.1. Nanorod Alignment and Optical Effects

The procedure reported herein for fabricating PVA films containing aligned gold nanorods was previously used by van der Zande et al.,[19] using nanorods prepared via electrochemical deposition within the pores of an alumina membrane, and by Mulvaney and co-workers[20] for silver nanorods. The method consists of drying a mixed aqueous solution of the nanorods and PVA, and subsequently warming up and stretching the composite film. Transmission electron microscopy (TEM) observations show (Fig. 1a) that, upon drying, the nanoparticles are randomly distributed within the film. Consequently, the optical properties of non-stretched films resemble those of the gold-nanorod precursor dispersion, displaying both longitudinal and transversal plasmon resonances independently of the polarization of the incident light, because all different orientations are probed. When the composite films are carefully warmed up and stretched, the gold nanorods tend to align in a preferred direction, as seen in the TEM image shown in Fig. 1b. This alignment is driven by the elongation of the PVA polymer molecules.[21,22]

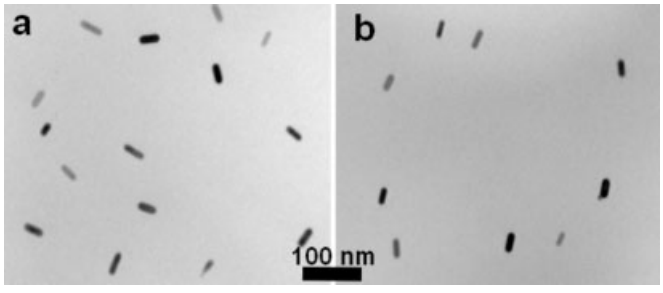

Figure 1. Transmission electron microscope images of PVA films containing gold nanorods before (a) and after (b) stretching.

This procedure works very well, as shown in Figure 1 and in the Supporting Information. After stretching, the optical response of the films becomes polarization-dependent. This optical effect is clearly shown in Figure 2, where we show the different colors of PVA films containing oriented gold nanorods from the same batch (aspect ratio of 2.23), placed parallel and perpendicular to the polarization direction induced by a polarizer placed on top. The parallel film appears blue, the perpendicular one reddish. These different colors arise from the selective excitation of the longitudinal and transverse plasmon modes of the nanorods, respectively.

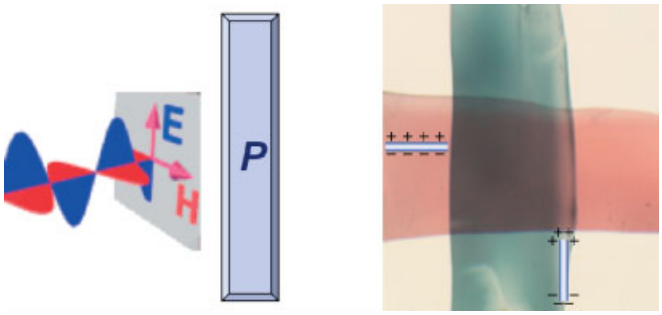

Figure 2. Photograph of PVA films containing gold nanorods aligned parallel (blue film) and perpendicular (red film) to the electric field of polarized incoming light as schematically shown on the left. The bar labelled P represents a polarizer.

The optical properties of small rods can be approximately described by means of a model derived by Gans for ellipsoids.[23] The polarizability of an ellipsoid is given by Equation 1

$$\alpha_{x,y,z} = \frac{4\pi\, abc\, (\varepsilon_{Au}-\varepsilon_m)}{3\varepsilon_m+3L_{x,y,z}(\varepsilon_{Au}-\varepsilon_m)} \quad (1)$$

where a, b, and c refer to the length of the ellipsoid along the x, y, and z axes ($a>b=c$), respectively, ε_{Au} is the dielectric function of gold, ε_m is the dielectric constant of the medium at optical frequencies, and $L_{x,y,z}$ is the depolarization factor for the respective axis, which is given by Equation 2

$$L_x = \frac{1-e^2}{e^2}\left(-1+\frac{1}{2e}\ln\frac{1+e}{1-e}\right);\; L_{y,z} = (1-L_x)/2 \quad (2)$$

where e is the rod ellipticity given by $e^2=1-(b/a)^2$. For a sphere, $e=0$ and $L=1/3$. The polarizability is related directly to the extinction of light by $C_{ext}=k\mathrm{Im}(\alpha)$. By using these equations, spectra can be calculated for varying aspect ratios and environments. These equations predict the presence of two distinct absorption bands for random orientation with respect to the

ADVANCED FUNCTIONAL MATERIALS

electric field of the incident light, which are usually attributed to parallel and perpendicular surface plasmon resonance modes of the nanorods.

The spectrum of an unstretched PVA film indeed displays two resonance peaks, and the same result is observed in the case of a stretched film under non-polarized light, since, though the rods are preferentially oriented in one direction, the incident light contains all orientations of the oscillating electric field, so that both plasmon modes are excited. However, when the spectrum is measured under light polarized parallel to the stretch direction of the film, the longitudinal plasmon band is selectively excited, whereas under light polarized perpendicular to the stretch direction, only the transverse mode is excited. This effect is exemplified in Figure 3, for nanocomposite films prepared with two different gold-nanorod samples of varying aspect ratios. In both cases, one can see two bands in the spectrum of the unstretched film, as well as complete suppression of one of them in each of the spectra measured under parallel or perpendicular polarization. This highlights the monodispersity and the high quality of the samples, as well as the high degree of alignment along the stretch direction. It is also clear that the rods are well-separated within the film, since otherwise there would be interactions between them, as has been demonstrated in the literature.[24,25]

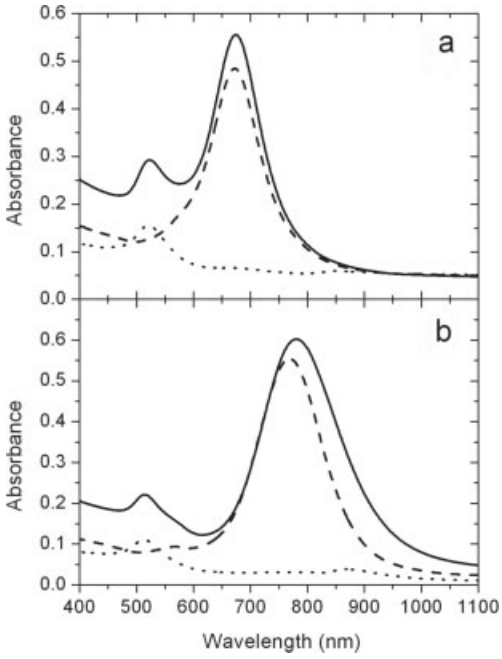

Figure 3. UV-vis-NIR spectra of PVA films containing gold nanorods: non-stretched (unbroken lines), stretched with parallel (dashed lines) and perpendicular polarization (dotted lines), for aspect ratios of a) 2.23 and b) 2.94.

More complete information can be obtained by measuring the absorption spectrum at various intermediate polarization angles, as shown in Figure 4. As the angle deviates from zero or ninety degrees, contributions from both plasmon modes are observed, and the fraction of each of them is related to the deviation from the respective orientation, as indicated by the presence of two, perfect, isosbestic points in Figures 4a,b. Such isosbestic points are predicted by the calculations of the optical

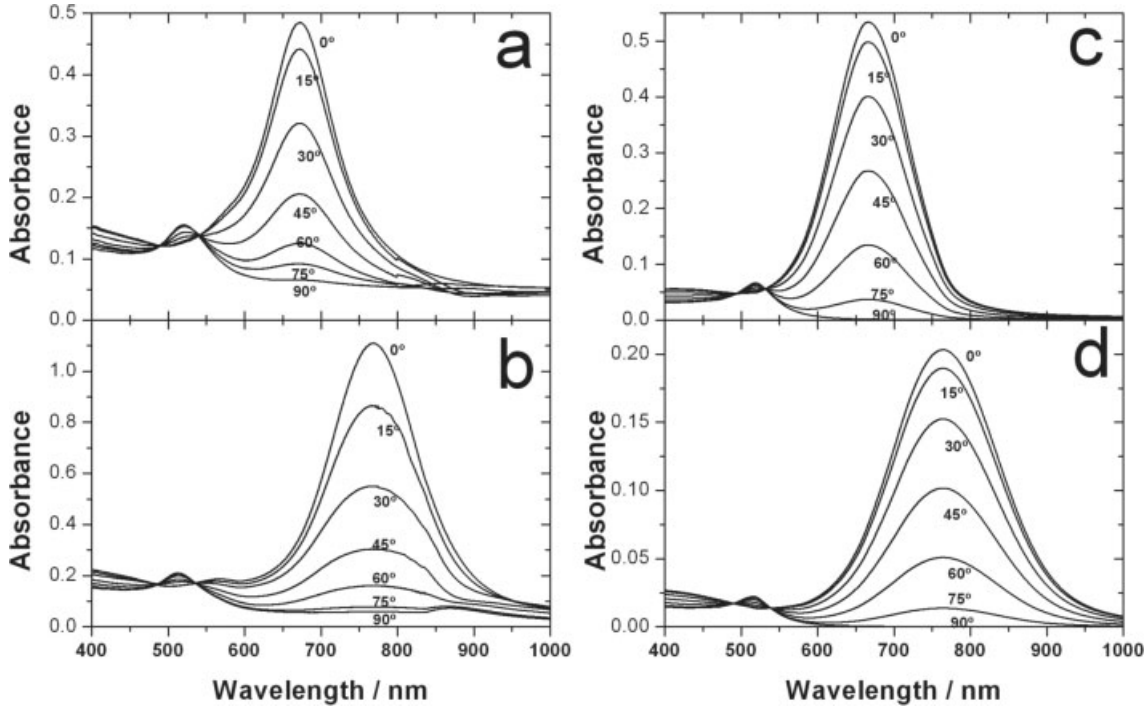

Figure 4. a,b) Experimental UV-vis-NIR spectra of stretched PVA films containing gold nanorods with two different aspect ratios—2.23 (a) and 2.94 (b)—for varying polarization angles, as indicated. c,d) Simulated spectra of gold nanorods in a matrix with a refractive index of 1.5. A fixed rod width of 10 nm and lengths of 23 ± 6 nm and 32 ± 8 nm, respectively, were assumed in the calculations.

response of prolate ellipsoids using the Mie–Gans equations (see Eq. 4 in the Experimental Sec.), as shown in Figures 4c,d. The calculated spectra assume a fixed width of 10 nm, while a Gaussian distribution of lengths was introduced to simulate the plasmon peak width. Values of 23 ± 6 nm and 32 ± 8 nm were found to accurately reproduce the experimental peak positions and widths.

A comparison between the measured experimental values (for two different aspect ratios) and those obtained using Equation 1 is shown in Figure 5, where we plotted the normalized absorbance difference at the maximum of the longitudinal plasmon band, calculated using Equation 3

$$\text{Normalized absorbance difference} = \frac{\text{Abs}(\theta) - \text{Abs}(90)}{\text{Abs}(0) - \text{Abs}(90)} \qquad (3)$$

In both cases, there is a small deviation from the calculated values, which can be attributed to deviations from perfect alignment of the nanorods inside the PVA films.

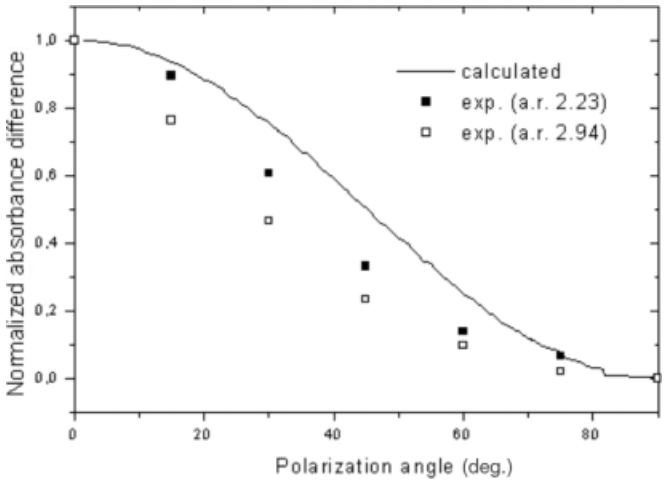

Figure 5. Plot of the measured absorbance of the film at the longitudinal surface plasmon peak position as a function of the polarization angle, and the fit using Equation 4. Experimental results for two different aspect ratios are plotted for comparison as the normalized absorbance difference (see text for details).

2.2. Patterning

Several groups have reported that non-spherical particles can undergo irradiation-induced shape and size transformations.[26,27] After irradiating a gold-nanorod dispersion with a nanosecond laser tuned at 532 nm, Chang et al. observed a damping of the longitudinal plasmon band and an enhancement of the band at 520 nm, indicating the disappearance of nanorods and an increase in the number of nanospheres in the dispersion through a photoannealing process.[26] They claimed that by absorbing this radiation the nanorods excited and accumulated phonon energy, which was responsible for the observed shape transition. Link et al. simultaneously reported the photothermal instability of colloidal gold nanorods under laser irradiation with different pulse-widths.[28–30] They found that when a gold-nanorod dispersion was irradiated with femtosecond laser pulses at 800 nm having pulse energies in the microjoule range, the nanorods melted selectively into nanodots with no fragmentation. Different results were obtained when a nanosecond laser pulse was used,[27–29] Under those conditions, the energy threshold for the complete melting of the nanorods was reduced by a factor of a hundred compared to femtosecond laser pulse excitation. Although all these studies were performed in aqueous solution, Mulvaney and co-workers recently demonstrated a similar effect during the irradiation of silver nanorods within PVA films with a 355 nm Nd:YAG nanosecond laser,[20] and were thereby able to melt nanorods within the irradiated area selectively. Despite the obvious macroscopic optical effects, there was no microscopic evidence of melting.

We have improved this process with PVA films containing oriented gold nanorods, and the first results are shown in Figure 6. Irradiation of a circular area of the film with a nanosecond laser beam leads to a noticeable color change, and the color of the irradiated area is insensitive to the polarization of incident light, indicating that the starting anisotropic nanorods have been converted into isotropic particles, presumably

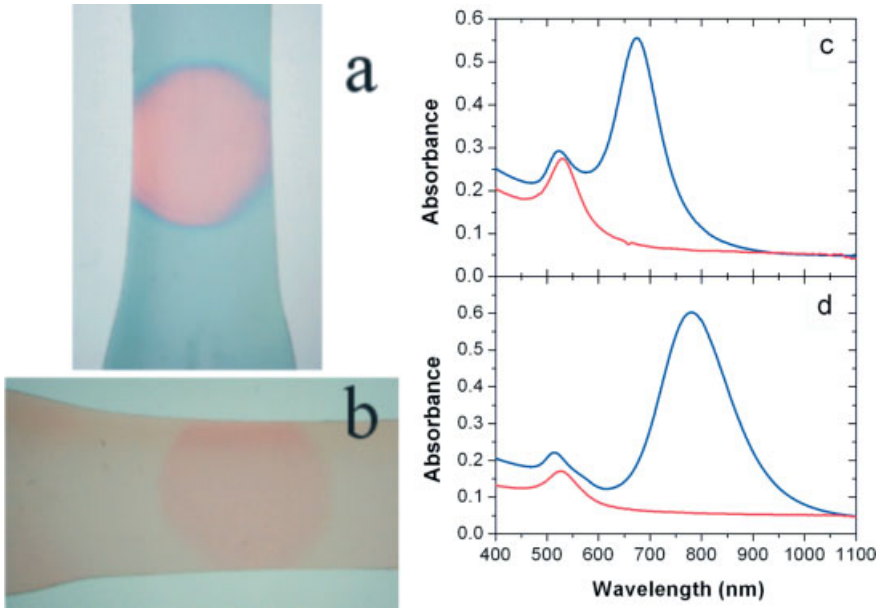

Figure 6. a,b) Photographs of PVA films containing gold nanorods aligned parallel (a) and perpendicular (b) to the electric field of polarized incoming light. The middle red spot was irradiated with a single pulse of a nanosecond laser. c,d) UV-vis spectra of the aligned films before (blue) and after (red) laser irradiation, for aspect ratios of 2.23 (c) and 2.94 (d).

ADVANCED FUNCTIONAL MATERIALS

spheres. This also agrees with a change in the shape of the UV-vis spectra, which show a single absorption band centered around 520 nm after irradiation, irrespective of the initial aspect ratio of the nanorods (Figs. 6c,d).

In order to confirm this speculation, we performed TEM studies on both non-irradiated and irradiated areas of two different films, initially containing aligned gold nanorods of different aspect ratios. Representative results are shown in Figures 7,8 for shorter and longer nanorods, respectively. It is obvious that, although the particles in the non-irradiated areas retain their original shape, upon irradiation they are converted into rather monodisperse spheres, thus confirming our initial assumption. TEM examination was also carried out at the edges between irradiated and non-irradiated areas, showing some particles with irregular shapes (Fig. 8c), indicating the sharp boundary between areas: some particles retain their original rod-like shape, others have been transformed into spheres.

Interestingly, TEM analysis reveals a clear decrease in the volume of the spheres obtained by laser irradiation—compared to the volume of the precursor nanorods. The extent of this volume reduction depends on the aspect ratio of the starting nanorods; it is more pronounced (up to 43 %) for rods with a higher aspect ratio (see Table 1). This decrease in particle volume is presumably related to the partial fragmentation of the particles during irradiation, which was often observed in the TEM images. Figure 7c shows a representative example, where small fragments can be clearly seen in the vicinity of the final spheres. Similar effects were previously observed by Wang et al.[26] and Nikoobakht and El-Sayed,[27] who suggested that the power of the laser pulse causes the nanorods to melt, accompanied by partial fragmentation. The narrow size distribution of the spherical nanoparticles suggests that homogeneous fragmentation of the nanorods is the likely pathway.

Table 1. TEM analysis of the nanoparticles before and after laser irradiation.

Aspect ratio	Length [nm]	Width [nm]	V_{rod} [a] [nm^3]	d_{sphere} [nm]	V_{sphere} [nm^3]
2.23 ± 0.30	37.3 ± 5.2	16.9 ± 2.3	11 643.77	25.9 ± 3.3	9090.36
2.94 ± 0.57	30.1 ± 3.5	10.5 ± 1.7	4027.10	16.3 ± 1.7	2277.19

[a] To calculate the nanorod volume, a cylindrical shape with hemispherical caps was assumed.

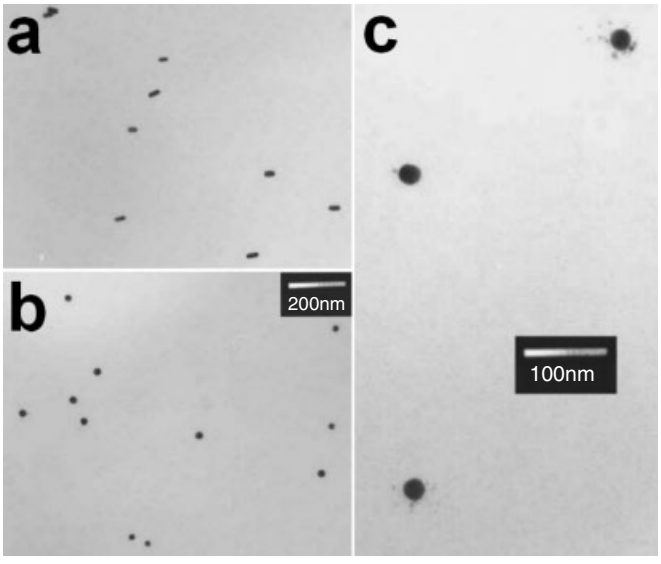

Figure 7. TEM images of PVA films containing aligned gold nanorods (aspect ratio = 2.23) before (a) and after (b) irradiating with a nanosecond laser. c) Higher magnification TEM image showing fragmentation of the particles.

This selective nanoparticle reshaping provides a clear opportunity to carry out micropatterning of the PVA nanocomposite films, simply by irradiating with a nanosecond laser through a suitable mask. For demonstration purposes, a 100 mesh copper TEM grid was employed. As shown in Figure 9, the shape of the grid is perfectly reproduced on the film, by the selective melting of rods in the areas that have been irradiated, leaving unchanged the areas "shaded" by the grid (some 30 μm thick in this case). The good definition observed in Figure 9c indicates that even smaller features could be "drawn" on these films if suitable templates were used. Figure 9 also shows that just by changing the polarization of incident light, the contrast between the irradiated and non-irradiated areas can be drastically changed, an effect which can be used for printing applications.

3. Conclusion

Thin films with uniform distributions of aligned gold nanorods of various aspect ratios can be easily prepared by drying nanorod dispersions in PVA solution, followed by stretching. The optical properties of such oriented films agree extremely well with predictions from Mie–Gans theory for small ellip-

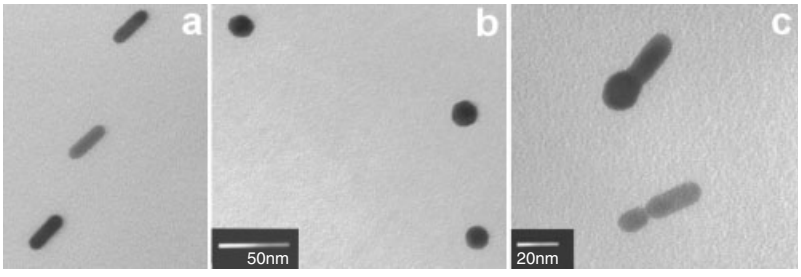

Figure 8. a,b) TEM images of PVA films containing aligned gold nanorods (aspect ratio = 2.94) before (a) and after (b) irradiating with a nanosecond laser. c) TEM of particles at the edge of the irradiated spot.

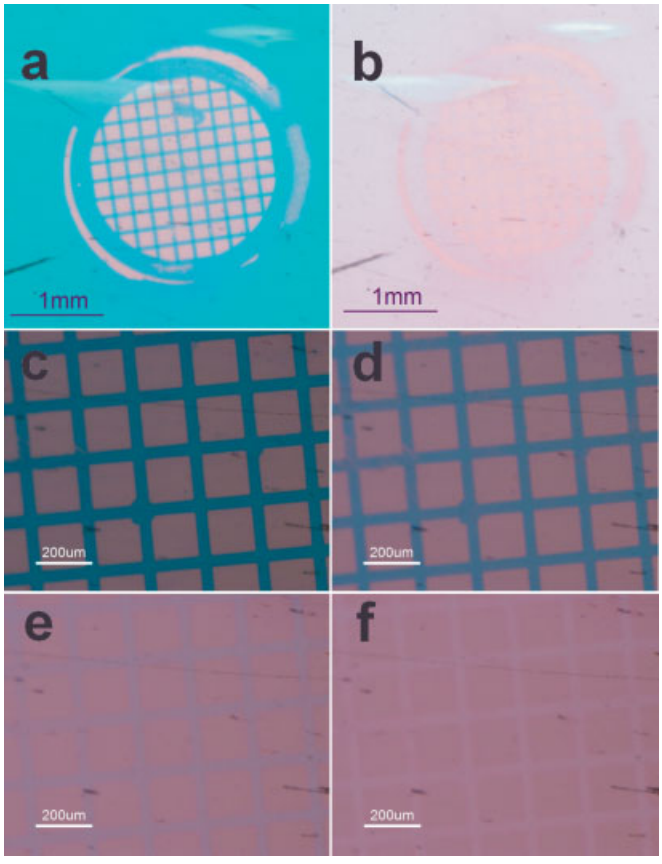

Figure 9. a,b) Photographs of a PVA film containing aligned gold nanorods (aspect ratio = 2.23), irradiated with a single pulse of a nanosecond laser using a TEM grid as a mask, illuminated under parallel (a) and perpendicular (b) polarization. c–f) Photographs of a selected area under 12× magnification and various polarization angles. An animated gif file is available in the Supporting Information.

soids when polydispersity is included in the calculations, so that selective excitation of each plasmon mode can be achieved using polarized light. Additionally, spatially resolved rod-to-sphere transitions can be induced by illumination with a nanosecond laser, which has been demonstrated by preliminary micropatterning experiments.

4. Experimental

Tetrachloroauric acid ($HAuCl_4 \cdot 3H_2O$), cetyltrimethylammonium bromide (CTAB), ascorbic acid, $NaBH_4$, $AgNO_3$, and PVA (weight-average molecular weight 70 000–100 000) were purchased from Aldrich. Milli-Q water with a resistivity higher than 18.2 MΩ cm was used in all the preparations.

Gold nanorods were prepared by a modified version of the seeding method of El-Sayed and co-workers [31,32]. Briefly, a seed solution was prepared by mixing an aqueous solution of $HAuCl_4$ (5 mL, 0.250 mM) with an ice-cold, freshly prepared $NaBH_4$ (0.3 mL, 10 mM) solution. To grow the gold nanorods, different amounts of the seed solution (0.06 and 0.12 mL) and $AgNO_3$ solution (0.05 and 0.08 mL, respectively, 5 mM) were added to a reaction mixture containing $HAuCl_4$ (0.1 mL, 50 mM), ascorbic acid (0.080, 0.075 mL, 100 mM), and CTAB (10 mL, 0.1 M). The aspect ratio of the rods increased as the amount of added seed solution increased and the amount of $AgNO_3$ decreased. TEM analysis of the gold nanorods revealed average aspect ratios of 2.23 ± 0.30 (length 37.3 ± 5.2 nm, width 16.9 ± 2.3 nm), and 2.94 ± 0.57 (length 30.1 ± 3.5 nm, width 10.5 ± 1.7 nm).

Thin films of gold nanorods dispersed in PVA were prepared by drying a nanorod colloid ($[Au] = 3.3 \times 10^{-4}$ M) in the presence of dissolved PVA (7.5 wt.-%). The nanorods were aligned by warming and stretching (by hand) the composite film. Care should be taken to avoid overheating, since this can lead to modification of the optical properties due to thermal reshaping of the rods.

TEM samples were prepared by sticking stripes (5 mm wide) of the PVA film to an epoxy resin (Struers EPOFIX). The dry stripes were then sliced in an ultramicrotome (Reichert Ultracut S), with a glass knife to a thickness of 75 nm, and deposited onto a Formvar-coated copper grid. Ultramicrotomed samples were imaged in a JEOL JEM 1010 transmission electron microscope at an acceleration voltage of 100 kV. Because of the irregularity in the thickness of the cut stripes, the spatial resolution and contrast of such images is limited.

UV-vis spectra of composite films were measured directly with a Cary 5000 UV-vis-NIR spectrophotometer using special holders for the samples and the polarizer.

Laser irradiation was performed by illuminating with a single pulse (6 ns) of a Nd:YAG nanosecond laser (Brilliant B) operating at a wavelength of 1064 nm and a pulse energy of 850 mJ. For micropatterning, a 100 mesh TEM copper grid was placed between the laser and the sample during irradiation.

The extinction coefficient of gold nanorods was calculated by means of Mie–Gans theory [33], assuming an ellipsoidal shape. For oriented, small nanorods, the extinction coefficient of the film is given by Equation 4

$$C_{ext} = k\mathrm{Im}\{\alpha_T(1-\cos^2(\theta)) + \alpha_L(\cos^2(\theta))\} \quad (4)$$

where k is the wave vector of the light in the medium and θ is the angle measured with respect to the major axis. The polarizability α along the longitudinal and transverse axes is calculated using the conventional ellipsoid model [33]. To allow for the polydispersity of the particle samples, a Gaussian distribution has been assumed. The primary effect of polydispersity is to reduce the peak intensity of the longitudinal surface plasmon mode; for severely broadened samples, there is a shift in the peak position to longer wavelengths, due to the higher extinction coefficient of longer rods.

Received: December 17, 2004
Final version: January 20, 2005
Published online: April 13, 2005

[1] W. A. Weyl, *Coloured Glasses*, Society of Glass Technology, Sheffield, UK **1951**.
[2] L. M. Liz-Marzán, *Mater. Today* **2004**, *6*, 26.
[3] P. Mulvaney, *Langmuir* **1996**, *12*, 788.
[4] U. Kreibig, M. Vollmer, *Optical Properties of Metal Clusters*, Springer-Verlag, Berlin, Germany **1996**.
[5] J. A. A. Perenboom, P. Wyder, F. Meier, *Phys. Rep.* **1981**, *78*, 173.
[6] L. M. Liz-Marzán, M. Giersig, P. Mulvaney, *Langmuir* **1996**, *12*, 4329.
[7] S. J. Oldenburg, R. D. Averitt, S. L. Westcott, N. J. Halas, *Chem. Phys. Lett.* **1998**, *288*, 243.
[8] C. R. Martin, *Science* **1994**, *266*, 1961.
[9] C. A. Foss, Jr., G. L. Hornyak, J. A. Stockert, C. R. Martin, *Adv. Mater.* **1993**, *5*, 135.
[10] N. R. Jana, L. Gearheart, C. J. Murphy, *Adv. Mater.* **2001**, *13*, 1389.
[11] J. Pérez-Juste, L. M. Liz-Marzán, S. Carnie, D. Y. C. Chan, P. Mulvaney, *Adv. Funct. Mater.* **2004**, *14*, 571.
[12] H. Kozuka, S. Sakka, *Chem. Mater.* **1993**, *5*, 222.
[13] J.-H. Gwak, S.-J. Kim, M. Lee, *J. Phys. Chem. B* **1998**, *102*, 7699.
[14] L. Armelao, R. Bertoncello, M. De Dominicis, *Adv. Mater.* **1997**, *9*, 737.

ADVANCED FUNCTIONAL MATERIALS

[15] Y. Kobayashi, M. A. Correa-Duarte, L. M. Liz-Marzán, *Langmuir* **2001**, *17*, 6375.
[16] B. Rodríguez-González, A. Sánchez-Iglesias, M. Giersig, L. M. Liz-Marzán, *Faraday Discuss., Chem. Soc.* **2004**, *125*, 133.
[17] V. I. Boev, J. Pérez-Juste, I. Pastoriza-Santos, C. J. R. Silva, M. J. M. Gomes, L. M. Liz-Marzán, *Langmuir* **2004**, *20*, 10268.
[18] Y. Dirix, C. Bastiaansen, W. Caseri, P. Smith, *Adv. Mater.* **1999**, *11*, 223.
[19] B. M. I. Van der Zande, L. Pages, R. A. M. Hikmet, A. Van Blaaderen, *J. Phys. Chem. B* **1999**, *103*, 5761.
[20] O. Wilson, G. J. Wilson, P. Mulvaney, *Adv. Mater.* **2002**, *14*, 1000.
[21] J. Michl, E. W. Thulstrup, J. H. Eggers, *J. Phys. Chem.* **1970**, *74*, 3878.
[22] D. Fornasiero, F. Grieser, *Chem. Phys. Lett.* **1987**, *139*, 103.
[23] R. Gans, *Ann. Phys.* **1912**, *37*, 881.
[24] M. Gluodenis, C. A. Foss, *J. Phys. Chem. B* **2002**, *106*, 9484.
[25] K. G. Thomas, S. Barazzouk, B. I. Ipe, S. T. S. Joseph, P. V. Kamat, *J. Phys. Chem. B* **2004**, *108*, 13 066.
[26] S.-S. Chang, C.-W. Shih, C.-D. Chen, W.-C. Lai, C. R. C. Wang, *Langmuir* **1999**, *15*, 701.
[27] S. Link, C. Burda, B. Nikoobakht, M. A. El-Sayed, *Chem. Phys. Lett.* **1999**, *315*, 12.
[28] S. Link, C. Burda, M. B. Mohamed, B. Nikoobakht, M. A. El-Sayed, *J. Phys. Chem. A* **1999**, *103*, 1165.
[29] S. Link, C. Burda, B. Nikoobakht, M. A. El-Sayed, *J. Phys. Chem. B* **2000**, *104*, 6152.
[30] S. Link, M. A. El-Sayed, *Int. Rev. Phys. Chem.* **2000**, *19*, 409.
[31] B. Nikoobakht, M. A. El-Sayed, *Chem. Mater.* **2003**, *15*, 1957.
[32] J. Pérez-Juste, M. A. Correa-Duarte, L. M. Liz-Marzán, *Appl. Surf. Sci.* **2004**, *226*, 137.
[33] C. F. Bohren, D. R. Huffman, *Absorption and Scattering of Light by Small Particles*, Wiley, New York **1983**.

